

Photo-neutron cross-section measurement in the 8 and 10 MeV bremsstrahlung induced reaction of ^{238}U

H. Naik · Rita Crasta · S. V. Suryanarayana · Ganesh Sanjeev · B. S. Shivashankar ·
H. G. Raj Prakash · N. Karunakara · H. M. Somashekarappa · M. Kumar ·
V. T. Nimje · K. C. Mittal · A. Goswami

Received: 28 January 2013 / Published online: 2 April 2013
© Akadémiai Kiadó, Budapest, Hungary 2013

Abstract The $^{238}\text{U}(\gamma, n)^{237}\text{U}$ reaction cross-section at the end point bremsstrahlung energies of 8 and 10 MeV was measured by using an activation technique. Induced gamma ray activities were measured by high resolution gamma-ray spectrometer with high-purity germanium detector. The photo neutron cross section on ^{238}U is also calculated theoretically using TALYS 1.2 computer code. The experimentally obtained reaction cross sections were compared with the flux weighted average values from the

literature data based on mono-energetic photon as well as the value from TALYS. It was found that the cross section of $^{238}\text{U}(\gamma, n)^{237}\text{U}$ reaction increases with increase of bremsstrahlung energy and were closer to the flux-weighted experimental data from literature and the values from TALYS based on mono-energetic photons.

Keywords $^{238}\text{U}(\gamma, n)^{237}\text{U}$ reaction cross-section · $^{238}\text{U}(\gamma, f)$ and $^{197}\text{Au}(\gamma, n)^{196}\text{Au}$ flux monitors · End point bremsstrahlung energies of 8 and 10 MeV · Off-line γ -ray spectrometric technique · TALYS 1.2 calculation

H. Naik (✉) · A. Goswami
Radiochemistry Division, Bhabha Atomic Research Centre,
Mumbai 400085, India
e-mail: naikhbarc@yahoo.com

R. Crasta · G. Sanjeev
Microtron Centre, Department of Studies in Physics,
Mangalore University, Mangalagangothri, Mangalore 574 199,
Karnataka, India

S. V. Suryanarayana
Nuclear Physics Division, Bhabha Atomic Research Centre,
Mumbai 400085, India

B. S. Shivashankar
Department of Statistics, Manipal University, Manipal 576 104,
Karnataka, India

H. G. Raj Prakash
Department of Engineering Physics, JNN College of
Engineering, Shimoga 577 204, India

N. Karunakara · H. M. Somashekarappa
University Science Instrumentation Centre, Mangalore
University, Mangalagangothri, Mangalore 574 199,
Karnataka, India

M. Kumar · V. T. Nimje · K. C. Mittal
Accelerator & Pulse Power Division, Bhabha Atomic Research
Centre, Mumbai 400085, India

Introduction

Nuclear data of photon-induced reactions play an important role both in applied research and in variety of applications [1]. The incident photons having energy below 30 MeV is the important region in most of the applications. This is because the giant dipole resonance reaction cross-sections of most of the reactions lie within incident energy range of 30 MeV. Natural uranium is a mixture of ^{238}U (99.2739 %), ^{235}U (0.7204 %), and ^{234}U (0.0057 %). The ^{235}U is a fissile material, whereas the ^{238}U is a non-fissile material, which plays an important role in nuclear reactors. The more abundant ^{238}U , capable of serving as a source material for the production of fissile ^{239}Pu in a nuclear reactors by neutron capture followed by two successive β -decays. Therefore ^{238}U is used as a source material for creating ^{239}Pu , which can be used as a nuclear fuel [2]. Thus nuclear reaction and fission data of ^{238}U are very important for fission, fusion and accelerator driven sub critical system (ADSs) calculations [3, 4]. In particular in ADSs, sufficient flux of high energy gamma photon in the form of bremsstrahlung is always produced along with the

neutrons. Thus the present work is focused to determine the photo-neutron cross-section of ^{238}U .

In published literature [5–7] number of experiments were carried out to calculate the $^{238}\text{U}(\gamma, n)^{237}\text{U}$ reaction cross-section. Most of the data available in published literature are for mono-energetic photons [8, 9] using linear accelerator facility. Gonzalez et al. [10] carried out the study of photo-neutron cross section of ^{238}U from 5.61 to 10.83 MeV, by using 30 different neutron capture gamma rays with high resolution in energy produced in an experimental arrangement at the IPEN-IEA-R12-MW research reactor. However, there is no data available in the literature using bremsstrahlung beam. In view of this, the present work was carried out to find the photo-neutron reaction cross-section of ^{238}U using the electron accelerator facility. The selected end-point energies of the bremsstrahlung were 8 and 10 MeV and the method used was activation technique followed by off-line γ -ray spectrometry. The $^{238}\text{U}(\gamma, n)^{237}\text{U}$ reaction cross-section induced by 8 and 10 MeV bremsstrahlung was also calculated theoretically using a TALYS 1.2 code [11] and the results were compared with experimental value of the present work.

Experimental procedure

The experiments were performed by using the bremsstrahlung beam with end point energies of 8 and 10 MeV, produced from 8 MeV Microtron accelerator at Mangalore university, Karnataka, India and 10 MeV electron linear accelerator (Linac) of the electron beam center, Kharghar, Navi-Mumbai, India. The salient features of the 8 MeV Microtron [12–14] and 10 MeV electron Linac [15, 16] are as follows:

| | Microtron | Electron Linac |
|-----------------------|-------------------|------------------|
| Beam Energy | 8 MeV | 10 MeV |
| Beam current | 50 mA | 100–200 mA |
| Pulse width | 2.5 μs | 10 μs |
| Pulse repetition rate | 250 Hz | 300–400 Hz |

In the Microtron accelerator, the bremsstrahlung beam with end point energy of 8 MeV was produced when a pulse electron hits a 0.188 cm thick tantalum target [14]. On the other hand in electron linac the bremsstrahlung beam with end point energy of 10 MeV was produced by impinging the electron beam on a 1 mm thick Ta target [15, 16]. In both the cases the Ta targets, which act as electron to photon converter were located at a distance of 3 cm from the beam exit window and the samples were

kept at a distance of 10 cm from the Ta target. The arrangement used for bremsstrahlung irradiation is shown in Fig. 1.

High-purity uranium metal foils of thickness 3.0363 and 1.6575 g/cm^2 weighing about 0.6587 and 0.9050 g were separately wrapped with 0.025 mm thick super pure aluminum foil and were irradiated separately by end point bremsstrahlung energies of 8 and 10 MeV, respectively. In the case of end point bremsstrahlung energy of 10 MeV, a 4.6007 g/cm^2 thick gold (Au) metal foil weighing 0.05434 g is separately wrapped with 0.025 mm thick super pure aluminum foil and was also irradiated along with the aluminum wrapped uranium metal foil. The Au foil was used as a monitor to find the bremsstrahlung flux. During the 8 MeV irradiation the Microtron accelerator was operated with a pulse repetition rate of 50 Hz, a pulse width of 2.42 μs and the average beam current of 33 mA. On the other hand, the electron linac was operated with a pulse repetition rate of 400 Hz, a pulse width of 10 μs and the average beam current of 50 mA. The irradiation time for the 8 and 10 MeV experiments were 3 and 4 h, respectively. The irradiated samples were cooled for sufficient time and then the gamma rays activities emitted from the activation foils were measured by using two different high purity germanium (HPGe) detectors. For 10 MeV bremsstrahlung irradiation experiment, the HPGe detector has a volume of 80 cm^3 and was coupled to a PC-based 4 K channel analyzer. On the other hand for 8 MeV bremsstrahlung irradiation experiment, the HPGe detector has a volume of 41.1 cm^3 and was coupled to a PC based 16 k channel analyzer. The energy resolution of the detector systems were 2.0 keV full width at half maximum (FWHM) at the 1332.0 keV peak of ^{60}Co . The cooling time and the measuring time were chosen based on the activity and the half-life of uranium and gold radionuclide. In order to optimize the dead time and the coincidence summing effect the appropriate distance between the sample and the detector was chosen for each of the measurements. The dead time of the detector system during counting was always kept as less than 10 %. The sample was counted for several times in order to obtain decay curves for the

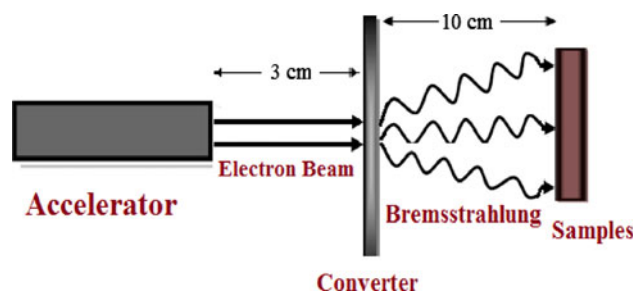


Fig. 1 The experimental arrangement of irradiation

photo-peaks as well as to observe the linearity of the experimental results. The typical γ -ray spectrum of the irradiated uranium and gold with bremsstrahlung is shown in Figs. 2 and 3, respectively. The activation products were identified based on γ -ray energies and half-life of radioactive isotopes.

Data analysis and results

Calculation of the photon flux

The net peak area (A_{net}) corresponding to the full energy peak was obtained from the total counts after subtracting the linear Compton background. In the case of end point energy of 10 MeV, the photon flux was calculated from the γ -ray activity of ^{196}Au obtained from the $^{197}\text{Au}(\gamma, n)^{196}\text{Au}$ reaction as well as from the γ -ray activity of the fission products ^{132}Te and ^{97}Zr from $^{238}\text{U}(\gamma, f)$ reaction using experimental yields (Y) from Ref. [16, 17]. On the other hand in the case of 8 MeV, the photon flux was calculated only from the γ -ray activity of fission products ^{132}Te and ^{97}Zr and using experimental yields (Y) in the bremsstrahlung induced fission of ^{238}U from Ref. [16, 17]. In the calculation of photon flux, the activity (A_{net}) of the γ -lines 228.1 keV of ^{132}Te and 743.4 keV of ^{97}Zr produced from the $^{238}\text{U}(\gamma, f)$ reaction and 355.7 keV of ^{196}Au from the $^{197}\text{Au}(\gamma, n)$ reaction were used. The following equation was used for the photon flux calculation:

$$\phi = \frac{A_{net}(CL/LT)\lambda}{N < \sigma > Y a \varepsilon (1 - e^{-\lambda t})(e^{-\lambda T})(1 - e^{-\lambda CL})}, \quad (1)$$

where N is the number of target atoms calculated from the exact weight of the target material. $< \sigma >$ is the flux weighted average value of $^{238}\text{U}(\gamma, f)$ and $^{197}\text{Au}(\gamma, n)^{196}\text{Au}$

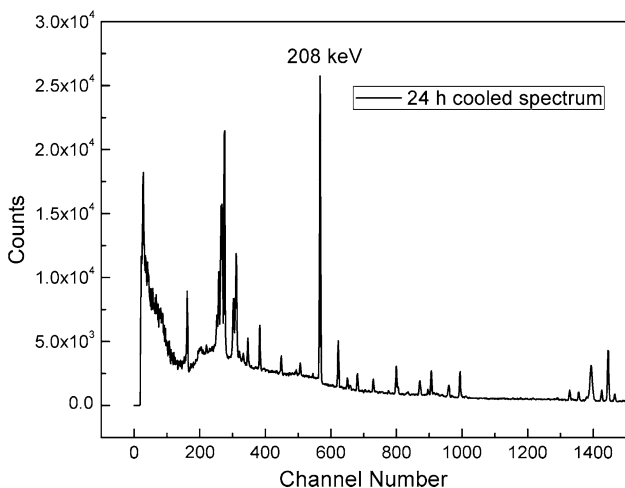


Fig. 2 Typical γ -ray spectrum from the activated ^{238}U foil with 10 MeV bremsstrahlung beam

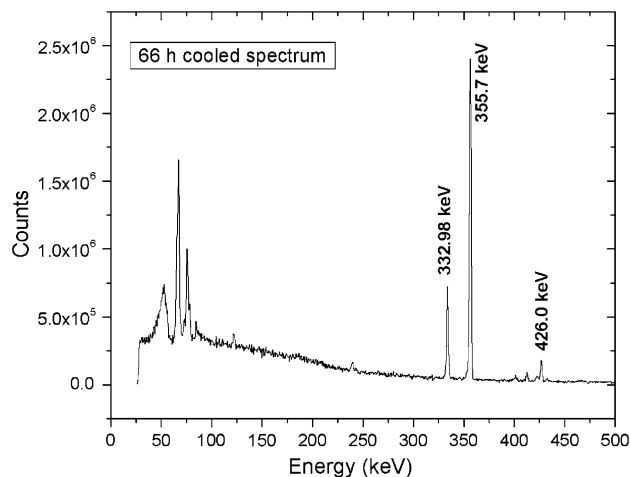


Fig. 3 Typical γ -ray spectrum from the activated ^{197}Au foil with 10 MeV bremsstrahlung beam

reaction cross-section respectively. ‘ Y ’ is the cumulative yield of the fission product ^{132}Te and ^{97}Zr . ‘ a ’ is the branching intensity of the γ - rays of the fission and activation products and ε is the detection efficiency of the γ - rays of interest. ‘ λ ’ is the decay constant of the isotope related to its half-life ($T_{1/2}$) as $\lambda = \ln 2/T_{1/2}$. ‘ t ’ and T are the irradiation and cooling times whereas, CL and LT are the clock time and live time of counting, respectively. In the above equation the CL/LT term has been used for dead time correction. The γ -ray energies and the nuclear spectroscopic data such as the half-lives and branching ratios of the fission products are taken from Refs. [18–20] and given in Table 1.

The flux weighted average cross-section ($< \sigma >$) for $^{238}\text{U}(\gamma, f)$ and $^{197}\text{Au}(\gamma, n)^{196}\text{Au}$ reactions were calculated using the relation

$$< \sigma > = \frac{\sum (\sigma \phi)}{\sum \phi} \quad (2)$$

where ϕ is the photon flux for $^{238}\text{U}(\gamma, f)$ and $^{197}\text{Au}(\gamma, n)^{196}\text{Au}$ reaction.

The photon flux (ϕ) as a function of photon energy was calculated by using GEANT4 code [21, 22]. GEANT4 is a

Table 1 Nuclear spectroscopy data used to obtain the reaction products: γ -ray energies, intensities and half-lives

| Nuclide | $T_{1/2}$ | E_{γ} (keV) | I_{γ} (%) | Reactions | E_{Th} (MeV) |
|-------------------|-----------|--------------------|------------------|------------------------------|----------------|
| ^{237}U | 6.75 d | 208.0 | 21.2 | $^{238}\text{U}(\gamma, n)$ | 6.1543 |
| ^{132}Te | 3.2 d | 228.1 | 88.0 | $^{238}\text{U}(\gamma, f)$ | 5.8 |
| ^{97}Zr | 16.91 h | 743.4 | 93.0 | $^{238}\text{U}(\gamma, f)$ | 5.8 |
| ^{196}Au | 6.183 d | 332.983 | 22.9 | $^{197}\text{Au}(\gamma, n)$ | 8.073 |
| | | 355.689 | 87 | | |
| | | 426.0 | 7 | | |

computer code and a toolkit for the simulation of the passage of particles through matter. In GANT4, there is a option to calculate the energy of photon (bremsstrahlung) from the interaction of electron with heavy-Z target like Ta, W, Th, U etc. However, during the calculation it needs to define the energy of the electron, the dimension of the target and its distance from the electron beam aperture. In our calculation, we have used GEANT4 code [21, 22] to generate the bremsstrahlung spectra by impinging electron beam energies of 8 and 10 MeV on a 1.88–1 mm thick Ta target with 5 cm × 5 cm area situated at a distance of 3 cm from the end of the electron beam exit. The bremsstrahlung spectra with end point energies of 8 and 10 MeV are shown in Fig. 4.

The values of $\langle \sigma \rangle$ for the end point bremsstrahlung energies of 8 and 10 MeV were calculated from the for $^{238}\text{U}(\gamma, f)$ reaction cross-section of literature data [8] for mono-energetic photon as well as from a theoretical value based on TALYS 1.2 [11] computer code (Fig. 5). For the same end point bremsstrahlung energy of 10 MeV, the $\langle \sigma \rangle$ value was also calculated for $^{197}\text{Au}(\gamma, n)^{196}\text{Au}$ reaction cross-section from the literature [23] and TALYS based on mono-energetic photons (Fig. 6). The flux-weighted average σ values for $^{238}\text{U}(\gamma, f)$ and $^{197}\text{Au}(\gamma, n)^{196}\text{Au}$ reactions from the literature as well as from TALYS are shown in Table 2. The $\langle \sigma \rangle$ value was used in Eq. (1) to calculate the photon flux (φ). The $^{238}\text{U}(\gamma, f)$, $^{197}\text{Au}(\gamma, n)^{196}\text{Au}$ and $^{238}\text{U}(\gamma, n)^{237}\text{U}$ reactions having different thresholds are presented in Table 1. Thus the weighted average flux obtained from $^{238}\text{U}(\gamma, f)$ and $^{197}\text{Au}(\gamma, n)^{196}\text{Au}$ reaction was multiplied by the flux ratio values of $^{238}\text{U}(\gamma, f)$ or $^{197}\text{Au}(\gamma, n)^{196}\text{Au}$ reaction from E_{th} to E_{max} to the $^{238}\text{U}(\gamma, n)^{237}\text{U}$ reaction from E_{th} to E_{max} . At the end point bremsstrahlung energy of 10 MeV, the

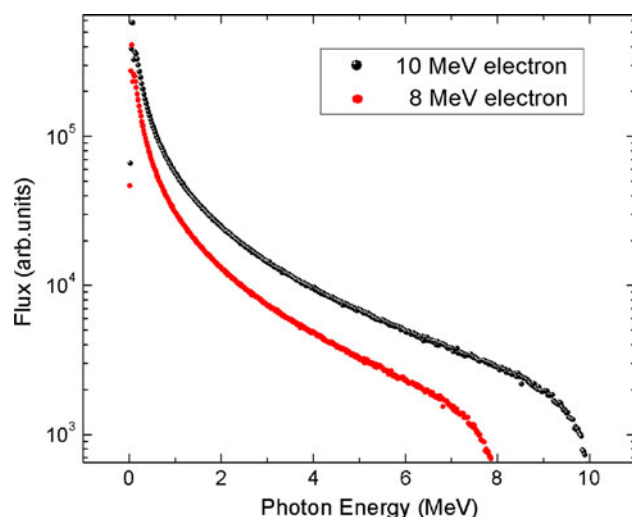


Fig. 4 Bremsstrahlung spectrum obtained by impinging electrons of 8 and 10 MeV energies

photon flux calculated from the activity of the fission products ^{132}Te and ^{97}Zr in $^{238}\text{U}(\gamma, f)$ and the reaction product ^{196}Au from the $^{197}\text{Au}(\gamma, n)^{196}\text{Au}$ reaction are in good agreement to each other. At the end point bremsstrahlung energy of 8 MeV the photon flux was calculated only from the activity of the fission products ^{132}Te and ^{97}Zr in $^{238}\text{U}(\gamma, f)$ reaction. This is because the threshold energy of $^{197}\text{Au}(\gamma, n)^{196}\text{Au}$ reaction is 8.073 MeV. Experimentally obtained photon fluxes in the above ways presented above are summarized in Table 2.

The $^{238}\text{U}(\gamma, n)^{237}\text{U}$ reaction cross section

The photon (bremsstrahlung) irradiation on ^{238}U resulted in the production of ^{237}U through (γ, n) reaction. The radio-nuclide ^{237}U from the $^{238}\text{U}(\gamma, n)$ reaction was identified by the photo-peak activity of the 208.0 keV characteristic γ -line from the γ -ray spectrum of a sufficiently cooled sample (Fig. 2). The decay data of the radio-active products, contributing reaction process and threshold energy are taken from the Ref. [20] and are presented in the Table 1.

The net activity under the photo-peak (A_{net}) of the reaction product ^{237}U was used to calculate the average photo neutron cross-section ($\langle \sigma \rangle$ of ^{238}U using the Eq. 1 and is rewritten as

$$\langle \sigma \rangle = \frac{A_{\text{net}} \left(\frac{CL}{LT} \right) \lambda}{N \phi a \varepsilon (1 - e^{-\lambda t}) (e^{-\lambda T}) (1 - e^{-\lambda CL})}. \quad (3)$$

All the terms have the similar meaning as in the Eq. (1) except φ which is the average flux for $^{238}\text{U}(\gamma, n)^{237}\text{U}$ reaction.

The $^{238}\text{U}(\gamma, n)^{237}\text{U}$ reaction cross-section determined in the present work at end point bremsstrahlung energies of 8 and 10 MeV are presented in Table 2. At 8 MeV, the

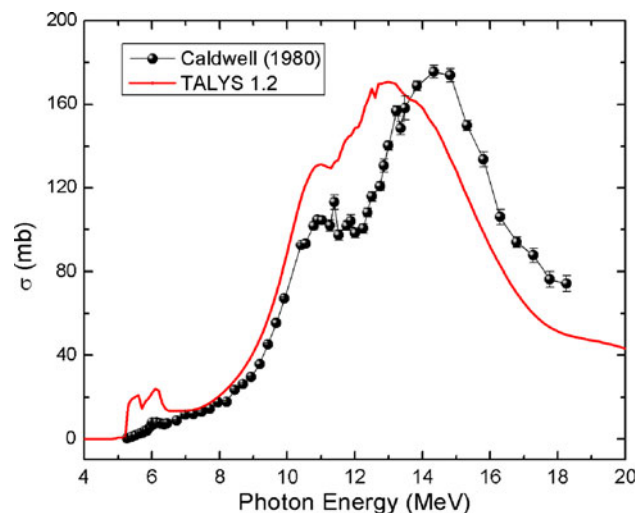


Fig. 5 Plot of experimental and theoretical $^{238}\text{U}(\gamma, f)$ reaction cross-section as a function of photon energy

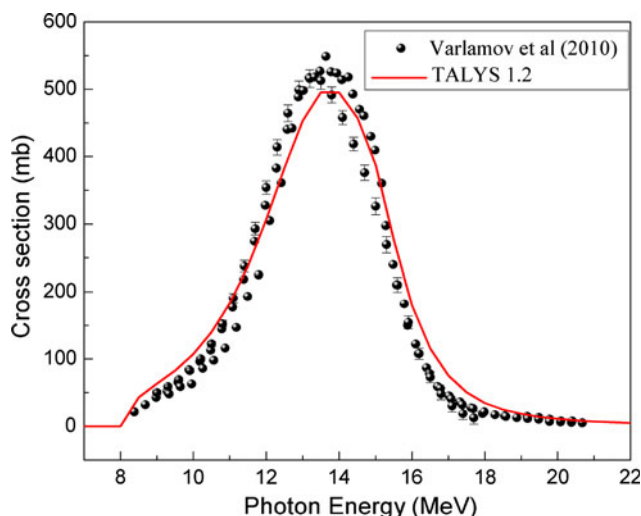


Fig. 6 Plot of experimental and theoretical $^{197}\text{Au}(\gamma, n)^{196}\text{Au}$ reaction cross-section as a function of photon energy

$^{238}\text{U}(\gamma, n)^{237}\text{U}$ reaction cross-section obtained to be 10.575 ± 0.16 mb for a bremsstrahlung flux of $(2.130 \pm 0.042) \times 10^9$ Photons/cm²/s using the flux weighted average value based on literature [8]. For the same energy using the flux weighted average value from the TALYS 1.2 code [11], the $^{238}\text{U}(\gamma, n)^{237}\text{U}$ reaction cross-section obtained as 22.467 ± 0.347 mb for a bremsstrahlung flux of $(1.003 \pm 0.020) \times 10^9$ Photons/cm²/s. Similarly, at 10 MeV, based on the flux weighted average value from literature [23], the $^{238}\text{U}(\gamma, n)^{237}\text{U}$ reaction cross-section obtained as 49.033 ± 0.191 mb for a bremsstrahlung flux of $(2.007 \pm 0.072) \times 10^9$ Photons/cm²/s. For the same energy using the flux weighted value of TALYS [11] the $^{238}\text{U}(\gamma, n)^{237}\text{U}$ cross section obtained as 69.776 ± 0.272 mb for a bremsstrahlung flux of 1.406 ± 0.0514 Photons/cm²/s. The range of $^{238}\text{U}(\gamma, n)^{237}\text{U}$ reaction cross-section for same end point bremsstrahlung energy is due to the use of two different types of photon flux based on experimental and theoretical $^{238}\text{U}(\gamma, f)$ and $^{197}\text{Au}(\gamma, n)^{196}\text{Au}$ reaction cross sections.

The uncertainties associated to the measured cross-sections come from the combination of two experimental data sets. The overall uncertainty is the quadratic sum of both statistical and systematic errors. The random error in the

observed activity is primarily due to counting statistics, which is estimated to be 5–10 %. This can be determined by accumulating the data for an optimum time period that depends on the half-life of nuclides of interest. The systematic errors are due to uncertainties in photon flux estimation (~3.6 %), the irradiation time (~0.5 %), the detection efficiency calibration (~3 %), the half-life of the reaction products and the γ -ray abundances (~2 %). Thus the total systematic error is about ~5.12 %. Thus the overall uncertainty is found to be in the range between 7.16 and 11.23 %, coming from the combination of a statistical error of 5–10 % and a systematic error of 5.12 %.

Discussions

The $^{238}\text{U}(\gamma, n)^{237}\text{U}$ reaction cross-section at an end point bremsstrahlung energies of 8 and 10 MeV shown in Table 2 are determined for the first time. It can be observed from the Table 2 that, the measured reaction cross section of $^{238}\text{U}(\gamma, n)^{237}\text{U}$ reaction based on 208.0 keV γ -line varies from 10.575 to 22.467 mb at 8 MeV to 49.033–69.776 mb at 10 MeV. The variation of the experimental and theoretical cross sections for both energies is due to the use of different types of photon flux based on experimental and theoretical flux weighted average cross section values of $^{238}\text{U}(\gamma, f)$ and $^{197}\text{Au}(\gamma, n)^{196}\text{Au}$ reactions.

In the published literature, number of experimental data were available to calculate the $^{238}\text{U}(\gamma, n)^{237}\text{U}$ reaction cross section using mono-chromatic photon beam but for the present investigation we have only considered the Ref. [8]. The authors in Ref. [8] calculated the $^{238}\text{U}(\gamma, n)^{238}\text{U}$ reaction cross-section in the Giant Dipole Resonance (GDR) region using the Livermore Linear accelerator facility and the photons produced in electron–positron annihilation. It can be seen from the literature data that the $^{238}\text{U}(\gamma, n)^{237}\text{U}$ reaction cross-section increase with increase of photon energy up to 11 MeV and thereafter decreases due to opening of other reaction channels. The higher $^{238}\text{U}(\gamma, n)^{238}\text{U}$ reaction cross-section within the photon energy of 10–12 MeV is due to GDR effect. In the present work the higher cross section at end point bremsstrahlung

Table 2 Measured reaction cross-section of $^{238}\text{U}(\gamma, n)^{237}\text{U}$ at end point bremsstrahlung energies of 8 and 10 MeV

| Bremsstrahlung energy (MeV) | Reaction used for flux calculation | Flux-weighted $\langle \sigma \rangle$ for $^{238}\text{U}(\gamma, f)$ and $^{197}\text{Au}(\gamma, n)$ reactions ($\langle \sigma \rangle$ (mb)) [Ref] | Flux (ϕ) $\times 10^9$ (Photons/cm ² /s) | Experimentally measured $^{238}\text{U}(\gamma, n)$ reaction cross-section ($\langle \sigma \rangle$ (mb)) |
|-----------------------------|------------------------------------|--|--|---|
| 8 | $^{238}\text{U}(\gamma, f)$ | 4.17 (Expt.) [8] | 2.130 ± 0.042 | 10.575 ± 0.163 |
| 8 | $^{238}\text{U}(\gamma, f)$ | 8.86 (TALYS) [11] | 1.003 ± 0.020 | 22.467 ± 0.347 |
| 10 | $^{197}\text{Au}(\gamma, n)$ | 38.65 (Expt.) [23] | 2.007 ± 0.072 | 49.033 ± 0.191 |
| 10 | $^{197}\text{Au}(\gamma, n)$ | 55.0 (TALYS) [11] | 1.406 ± 0.051 | 69.776 ± 0.272 |

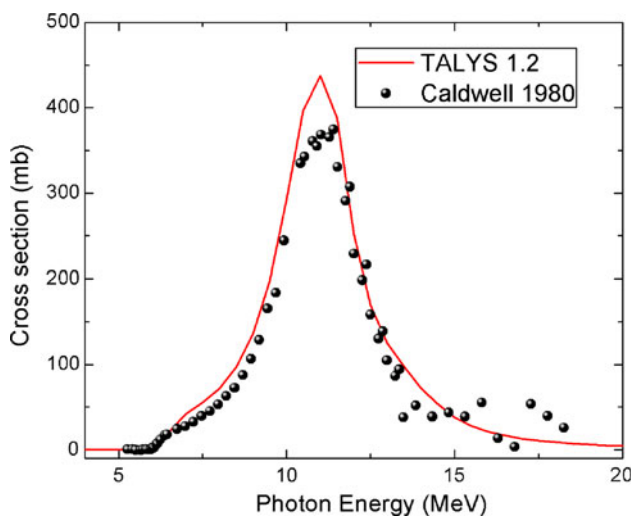


Fig. 7 Plot of experimental and theoretical $^{238}\text{U}(\gamma, n)^{237}\text{U}$ reaction cross-section as a function of photon energy

energy of 10 MeV is most probably due to the GDR effect. To observe the effect of GDR, the photo-neutron reaction cross section of ^{238}U as a function of photon energy from the literature [8] is plotted in the Fig. 7. It can be seen from Fig. 7 that, the $^{238}\text{U}(\gamma, n)^{237}\text{U}$ reaction cross section increases with photon energy from threshold to 12 MeV and thereafter decreases up to 18 MeV. From Fig. 7, the flux weighted $^{238}\text{U}(\gamma, n)^{237}\text{U}$ reaction cross-sections at end point bremsstrahlung energy of 8 and 10 MeV are calculated using Eq. 2 and are given in Table 3 along with the experimental data for comparison. The photon flux as function of energy was taken from Fig. 4. It can be seen from the Table 3 that, the experimentally determined $^{238}\text{U}(\gamma, n)^{237}\text{U}$ reaction cross section at 8 and 10 MeV bremsstrahlung energies based on 208.0 keV γ -line from the present investigation is closer to the flux-weighted value obtained from the available literature data which, shows the correctness of the present approach.

The $^{238}\text{U}(\gamma, n)^{237}\text{U}$ reaction cross sections at different photon energies above photo-neutron threshold of $^{238}\text{U}(\gamma, n)$ reaction were also calculated theoretically using nuclear model based computer code TALYS 1.2. TALYS [11] can be used to calculate the reaction cross-section based on physics models and parameterizations. It calculates nuclear

Table 3 Comparison of $^{238}\text{U}(\gamma, n)^{237}\text{U}$ reaction cross-section obtained from the bremsstrahlung spectrum of end-point energies of 8 and 10 MeV and flux-weighted average of mono-energetic photon

| Bremsstrahlung energy (MeV) | Experimental cross-section (mb) | Cross-section using literature [Ref. 8] (mb) | Cross-section using TALYS (mb) |
|-----------------------------|---------------------------------|--|--------------------------------|
| 8 | 10.575–22.467 | 16.752 | 23.318 |
| 10 | 49.033–69.776 | 48.390 | 63.860 |

reactions involving targets with mass larger than 12 amu and projectiles like photon, neutron, proton, ^2H , ^3H , ^3He and alpha particles in the energy range of 1–200 MeV. In the present work, we calculated the photo-neutron cross section of ^{238}U within energy range of 6.15–20 MeV using the default option in the TALYS code as done earlier in Refs [24, 25]. This is because the threshold energy of $^{238}\text{U}(\gamma, n)$ reaction is 6.15 MeV. All possible outgoing channels for a given projectile (photon) energy were considered including fission channel. However, the cross-section for the (γ, n) reaction was specially looked for and collected. Theoretically calculated $^{238}\text{U}(n, \gamma)$ reaction cross-section within photon energy of 6.15–20 MeV using TALYS is also plotted in Fig. 7.

It can be seen from Fig. 7 that the $^{238}\text{U}(\gamma, n)^{237}\text{U}$ reaction cross-section as a function of photon energy from TALYS 1.2 is in close agreement with the literature data. However, the value from TALYS shows a slight shift at the lower photon energy side and then it follows the path of experimental data. The flux weighted average $^{238}\text{U}(\gamma, n)^{237}\text{U}$ reaction cross section at end point bremsstrahlung energies of 8 and 10 MeV were also calculated from TALYS and are given in Table 3. It can be seen from the Table 3 that, the experimentally determined $^{238}\text{U}(\gamma, n)^{237}\text{U}$ reaction cross section at end point bremsstrahlung energies of 8 and 10 MeV from the present work is closer to the flux-weighted value obtained from TALYS 1.2 computer code as well as from the available literature data. It can be also observed from the experimental data of present work that the $^{238}\text{U}(\gamma, n)^{237}\text{U}$ reaction cross section increases from the end point bremsstrahlung energy of 8–10 MeV and follows a similar trend with the flux-weighted value obtained from the literature and TALYS 1.2 data based on the mono-energetic photons. The increase trend of experimental and calculated $^{238}\text{U}(\gamma, n)^{237}\text{U}$ reaction cross section with increase of end-point bremsstrahlung energy indicates the role of excitation energy besides the GDR effect.

Conclusion

- (i) The photo-neutron cross section of ^{238}U determined at an end point bremsstrahlung energies of 8 and 10 MeV for the first time using activation and off-line gamma ray spectrometric technique
- (ii) The $^{238}\text{U}(\gamma, n)^{237}\text{U}$ reaction cross-sections as a function of photon energy were calculated theoretically using computer code TALYS 1.2 version. The flux-weighted average cross-section for $^{238}\text{U}(\gamma, n)^{237}\text{U}$ reaction at the end point bremsstrahlung energies of 8 and 10 MeV have been obtained from the values of TALYS and literature data based on mono-energetic photon

- (iii) The experimentally determined $^{238}\text{U}(\gamma, n)^{237}\text{U}$ reaction cross-section at end point bremsstrahlung energies of 8 and 10 MeV were closer to the flux weighted value of TALYS as well as literature data. Both the experimental and flux-weighted $^{238}\text{U}(\gamma, n)^{237}\text{U}$ reaction cross-section increases from the end point bremsstrahlung energies of 8 to 10 MeV

Acknowledgments The authors are thankful to the staff of Microtron facility at Mangalagotri University, Mangalore, India for providing the electron beam to carry out the experiment.

References

- IAEA-TECDOC-1178. Hand book on photonuclear data for applications Cross- sections and spectra. Available online at: <http://www-nds.iaea.org>
- IAEA Nuclear Energy Series No.NF-T-4.1. Status and trends of nuclear fuels technology for sodium cooled fast reactors
- Nifenecker H, David S, Loiseaux JM, Meplan O (2001) Nucl Instr Methods Phys Res 463:428
- Ganesan S (2007) PRAMANA J Phys 68:257
- Veyssiere A, Beil H, Bergere R, Carlos P, Lepretre A, Kernbath K (1973) Nucl Phys A 199:45
- Mafra OY, Kuniyoshi S, Goldemberg J (1972) Nucl Phys A 186:110
- Mafra OY, Cesar MF, Renner C, Goldemberg J (1974) Nucl Phys A 1:236
- Caldwell JT, Dowdy EJ, Berman BL, Alvarez RA, Meyer P (1980) Phys Rev C 21:1215
- Dickey PA, Axel P (1975) Phys Rev Lett 35:501
- Gonçalez OL, Geraldo LP, Semmler R (1999) Nucl Sci Eng 132:135
- Koning AJ, Hilaire S, Duijvestijn MC (2005) TALYS: comprehensive nuclear reaction modeling. In: Haight RC, Chadwick MB, Kawano T, Talou P (eds) Proceedings of the international conference on nuclear data for science and technology-ND 2004, AIP vol 769. Santa Fe, USA, pp 1154–1159
- Siddappa K, Ganesh, Balakrishna KM, Ramamurthi SS, Soni HC, Shrivastava P, Sheth Y, Hemnani R (1998) Radiat Phys Chem 51:441
- Ganesh, Prashanth KC, Nagesh YN, Gnana Prakash AP, Umakanth D, Pattabi M, Siddappa K, Salkalachen S, Roy A (1999) Radiat Phys Chem 55:461
- Eshwarappaa KM, Ganesh, Siddappa K, Kashyap Yogesh, Sinha Amar, Sarkar PS, Godwal BK (2005) Nucl Instrum Methods Phys Res A 540:412
- Naik H, Nimje VT, Raj D, Goswami A, Sarbjit Singh, Acharya SN, Mittal KC, Ganesan S, Manchanda VK, Venugopal V (2009) Proceedings of the International Symposium on Nuclear Physics 348–349
- Naik H, Nimje VT, Raj D, Suryanarayana SV, Goswami A, Singh Sarbjit, Acharya SN, Mittal KC, Ganesan S, Chandrachoodan P, Manchanda VK, Venugopal V, Banarje S (2011) Nucl Phys A 853:1
- Pomme S, Jacobs E, Persyn K, De Frenne D, Govaert K, Yoneama M-L (1993) Nucl Phys A 560:689
- Brown E, Firestone RB (1986) In: Shirley VS (ed) Table of radioactive isotopes. Wiley, New York; Firestone RB, Ekstrom LP (2004) Table of radioactive isotopes. Version 2.1, Lawrence Berkeley National Laboratory, Berkeley [<http://ie.lbl.gov/toi/index.asp>]
- Blachot J, Fiche C (1981) Ann Phys Suppl 6:3
- Akovali YA (1995) Nucl Data Sheets 74:461
- Agostinelli S et al (2005) Nucl Instrum Methods A 506:250
- Allison J et al (2005) IEEE Trans Nucl Sci 53:270
- Varlamov VV, Ishkhanov BS, Orlin VN, SYu Troshchiev (2010) Izv. Rossiiskoi Akademii Nauk, Ser.Fiz. 74:884
- Naik H, Singh S, Goswami A, Manchanda VK, Kim G, Kim KS, Lee MW, Md S Rahman, Raj D, Ganesan S, Suryanarayana SV, Cho MH, Namkung W (2011) Nucl Instrum Methods Phys Res B 269:1417
- Crasta Rita, Naik H, Suryanarayana SV, Prajapati PM, Jagadisan KC, Thakare SV, Ganesh S, Nimje VT, Mittal KC, Goswami A (2011) J Radioanal Nucl Chem 290:367